Detection of Ground Surface Deformation Caused by the 2016 Kumamoto Earthquake by InSAR using ALOS-2 Data

Basara MIYAHARA, Yuji MIURA, Yasuaki KAKIAGE, Haruka UESHIBA, Masaki HONDA, Hiroyuki NAKAI, Tatsuya YAMASHITA, Yu MORISHITA, Tomokazu KOBAYASHI and Hiroshi YARAI

(Published online: 28 December 2016)

Abstract

SAR interferometry (InSAR) analysis of operational L-band SAR satellite of Japan, ALOS-2, reveals a series of coseismic crustal deformations caused by the 2016 Kumamoto Earthquake (April 14-16, 2016). Large coseismic deformation of over 10 centimeters due to the two large foreshocks and over 2 meters due to the mainshock can be clearly identified on the SAR interferograms as well as postseismic deformation up to a few centimeters. These displacements are concentrated around Futagawa-Hinagu fault zone which is a known active fault in Kyushu Island. 2.5-D displacements, more specifically quasi-east-west and quasi-vertical displacements due to the mainshock are also estimated from two interferograms observed from both east and west directions. The estimated displacements are consistent with those of ground GNSS observations. The sequence of the earthquakes causes significant distortion in the geodetic datum of Japan around the focal area, and thus positions of geodetic control points, which are fundamental infrastructure for implementing the datum needed to be revised as soon as possible. The area of the deformation could be promptly identified from the interferograms, and the control points which needed to be revised were quickly determined from the interferograms without any additional ground observation.

1. Introduction

The 2016 Kumamoto Earthquake (hereinafter referred as "the Kumamoto Earthquake") which occurred at 01:25 Japan Standard Time (JST) on April 16, 2016 caused huge crustal deformation in a wide area of the Kumamoto region, Kyushu Island, Japan. The deformation is complicated especially around the source fault zone, and it is almost impossible to reveal detailed spatial distribution of the deformation only from ground-based observations such as GNSS and geodetic leveling. Thus, synthetic aperture radar (SAR) interferometry (InSAR) analyses was conducted with respect to L-band SAR images observed by the Advanced Land Observing Satellite 2 (ALOS-2) which was launched by the Japan Aerospace Exploration Agency (JAXA) in May 2014. ALOS-2 has three advantages in observing ground surface deformation caused by earthquakes. The first advantage is the wavelength of the microwave. ALOS-2 is currently the only operational L-band SAR satellite. Generally speaking, L-band InSAR has a clear advantage in detecting ground surface displacements especially in vegetated areas compared with C- or X-band microwaves due to its high coherence (Kobayashi et al. 2011). In an area largely covered by vegetation like Japan, this capability is essential to capture the entire crustal deformation. The second advantage is a right-and-left looking observation capability. Using this right-and-left looking observations from both ascending and descending orbits, surface deformation can be measured from three or more directions and deformation analysis is available not only in 2.5-D (Fujiwara et al. 2000) but also in full 3-D (Morishita et al. 2016) when observation data from multi-directions is available. The third is highly frequent observations over a short period of time. In the Kumamoto Earthquake, the two large foreshocks occurred on April 14 and 15, and the mainshock on April 16. In addition, aftershocks and related earthquakes occurred frequently over relatively long duration in a wide area (JMA 2016).

The frequently repeated observations over a short period of time by ALOS-2 enabled effective monitoring of the deformation caused by the sequence of earthquakes. With these advantages, ALOS-2 contributes to detect the detailed crustal deformation caused by the Kumamoto Earthquake.

The Geospatial Information Authority of Japan (GSI) promptly requested JAXA to start emergency observations over an area around the epicenter using ALOS-2, and processed all of the observed data as soon as possible. This paper includes a report on the crustal deformations caused by the Kumamoto Earthquake as inferred from L-band InSAR analysis of ALOS-2.

2. Emergency Observation of ALOS-2

JAXA started emergency observations using ALOS-2 immediately after the two foreshocks, and continued with the frequent observations until the activity of the earthquake became sufficiently small, which was approximately a month. Table 1 shows a list of these observations. Per total, 18 observations were conducted and all the data was processed.

3. InSAR Analysis of ALOS-2

All the data of ALOS-2 emergently observed after the Kumamoto Earthquake was processed. Table 1 shows a list of the analyzed pairs of the SAR images. The processing software which was used is GSISAR. Tropospheric delay consisting of interferometric phases was estimated from a 5 km gridded numerical weather model provided by Japan Metrological Agency (JMA) and removed from the interferograms to reduce errors

Table 1 List of analyzed ALOS-2 images.

Pair no.	EQ	Acquisition date master image	Acquisition date slave image	Time (JST)	Flight direction	Looking direction	Obs. mode	Incidence angle at scene center (°)	Bp (m)
1	F	Nov. 14, 2014	April 15, 2016	12:53	Des.	Left	U-U	32.4	−104
2	F,M	May 18, 2015	April 18, 2016	00:25	Asc.	Right	U-U	50.7	+175
3	F,M	Mar. 07, 2016	April 18, 2016	12:18	Des.	Right	U-U	36.3	−124
4	F,M	Feb. 10, 2015	April 19, 2016	00:46	Asc.	Right	V-V	65.9	+54
5	F,M	Jan. 26, 2016	April 19, 2016	23:30	Asc.	Left	W-W	43.6	−186
6	F,M	Jan. 14, 2015	April 20, 2016	12:59	Des.	Left	U-U	43.0	−3
7	F,M	Dec. 04, 2015	April 22, 2016	00:11	Asc.	Right	H-H	34.0	−147
8	F,M	Mar. 30, 2016	April 27, 2016	00:18	Asc.	Right	U-U	43.0	−228
9	F,M	April 13, 2016	April 27, 2016	12:11	Des.	Right	U-U	42.9	+213
10	F,M	April 30, 2015	April 28, 2016	00:39	Asc.	Right	U-U	63.3	−154
11	M	April 15, 2016	April 29, 2016	12:52	Des.	Left	U-U	32.5	−152
12	M	April 15, 2016	April 29, 2016	23:44	Asc.	Left	U-U	24.5	+195
13	A	April 17, 2016	May 01, 2016	00:04	Asc.	Right	U-U	20.1	−171
14	A	April 17, 2016	May 01, 2016	11:57	Des.	Right	U-U	60.1	−89
15	A	April 18, 2016	May 02, 2016	12:18	Des.	Right	U-U	36.3	+87
16	A	April 22, 2016	May 06, 2016	00:11	Asc.	Right	H-H	34.0	+55
17	A	April 27, 2016	May 11, 2016	00:18	Asc.	Right	U-U	43.0	+362
18	A	May 02, 2016	May 16, 2016	12:18	Des.	Right	U-U	36.3	+157

Letters in column EQ represent interferograms that include F: before the mainshock (April 16, 2016, M 7.3), foreshocks only; M: the date of the mainshock; and A: after the mainshock only. Des and Asc stand for descending and ascending orbits, respectively. Letters H, U, V and W indicate Stripmap (6 m resolution), Stripmap (3 m resolution), ScanSAR (490 km swath) and ScanSAR (350 km swath) modes, respectively. Numbers in column Bp represent perpendicular baselines.

caused by atmosphere (Kobayashi et al., 2014). Stations coordinates of GNSS Earth Observation Network (GEONET) were utilized for mitigation of errors in long wavelength components such as ionospheric delay and satellite orbit errors (Morishita, 2016).

Figures 1 and 2 show SAR interferograms which indicate detected surface displacements caused by the two foreshocks and the mainshock respectively. The master image of Figure 1 was observed before the foreshocks and the slave image was observed after the foreshocks. The two foreshocks caused approximately 9cm displacement close to the satellite at the northwest side of the Futagawa fault zone and 12cm displacement away from the satellite at the southwest side of the fault zone (Fig. 1). The displacements detected by InSAR were utilized for estimation of a mechanism of the source fault, and the deformation is well explained by an almost pure dextral strike-slip fault with approximately 70 degree down dip to west (Kobayashi, 2016).

The mainshock caused huge displacements over 2 m along both Futagawa and Hinagu fault zones (Fig.2). The master image was observed before the mainshock and the slave image was observed after the mainshock.

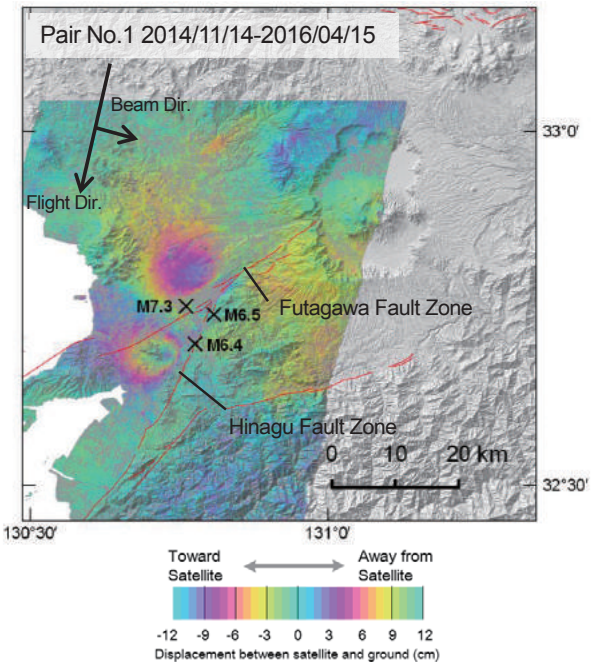

Fig. 1 SAR interferogram of pair No. 1. Black crosses indicate epicenters of the two foreshocks and mainshock. Red lines indicate estimated active faults (HERP, 2013).

Clear displacements including large deformations in Aso Caldera are also shown on an extension of east side of the already known Futagawa fault zone. These displacements are consistent with a dextral strike-slip fault mechanism.

SAR interferograms of ALOS-2 also detected postseismic displacements caused by the Kumamoto Earthquake. A-few-centimeter displacements away from the satellite are shown along the Futagawa fault zone and in Aso Caldera in both ascending and descending orbits (Fig. 3). This indicates subsidence is dominant in the postseismic phase.

4. 2.5-D Displacement Detected by ALOS-2

2.5-D coseismic displacements, more specifically quasi-east-west and quasi-vertical displacements of the mainshock were estimated from the two SAR interferograms shown in Figure 2, pairs No. 3 and 4. Figure 4 shows estimated 2.5-D displacement fields. On-site GNSS observations were also promptly conducted just 6 days after the earthquake in order to check accuracy of the 2.5-D displacement fields. Although only three points are available for comparison between InSAR and GNSS observations, the 2.5-D displacements are consistent with those measured through the on-site GNSS observations (Table. 2).

5. Summary and Concluding Remarks

SAR interferograms of ALOS-2 provided spatial distribution of the detailed coseismic deformations caused by the Kumamoto Earthquake. The coseismic displacements of up to 12cm were detected after the two foreshocks, and displacements over 2 m were clearly seen after the mainshock. In addition, a-few-centimeter significant postseismic displacements were also detected. These displacements were promptly detected by fully taking advantage of the ALOS-2 performance, and the information was utilized in understanding and estimating the mechanism of the earthquake source faults. The areas of the displacements were promptly identified from the SAR interferograms, and the information was directly utilized for determining control points which needed to be revised.

InSAR has become an essential tool to monitor

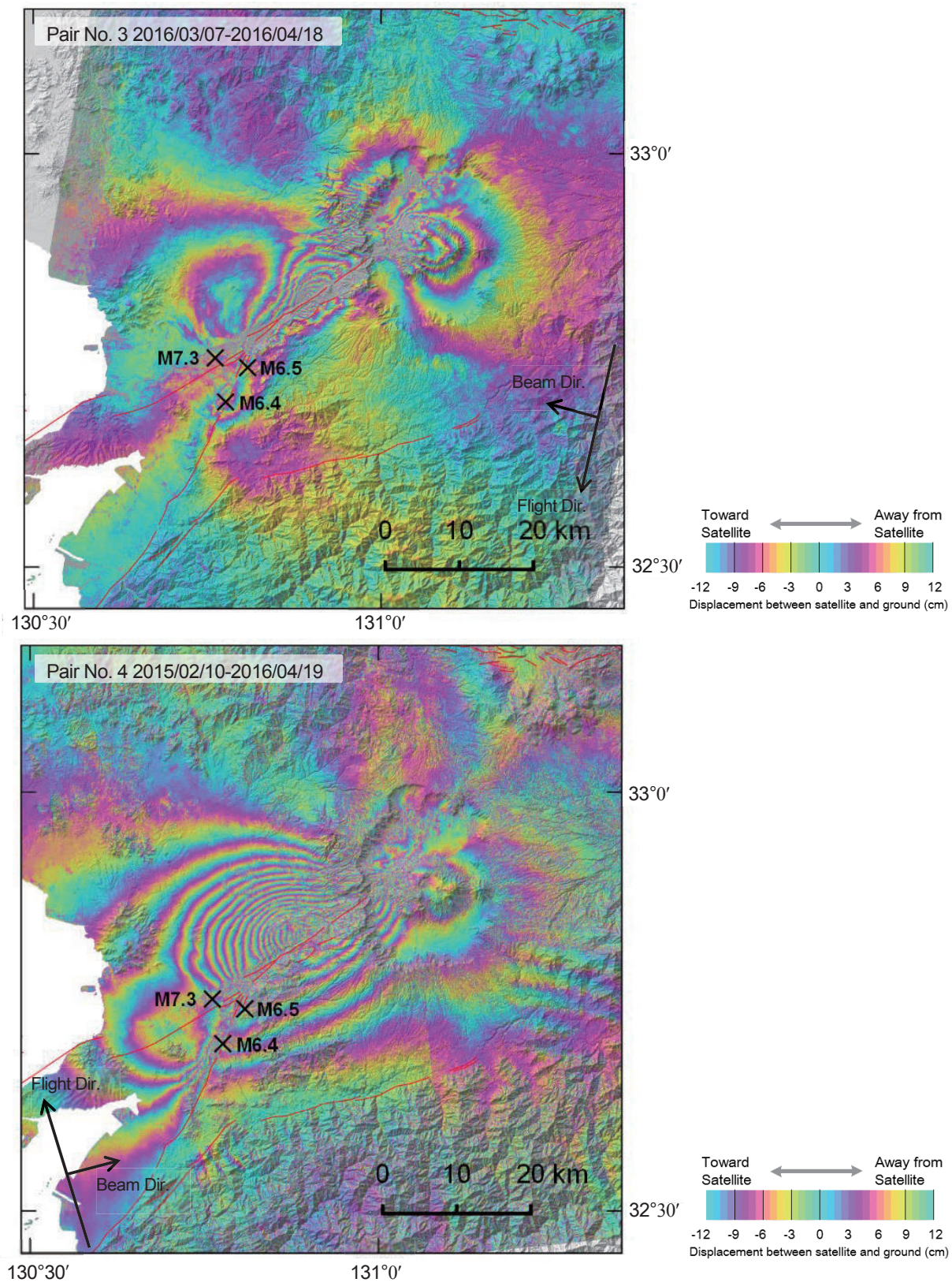

Fig. 2 SAR interferograms of pair No. 3 and No. 4. Black crosses indicate epicenters of the two foreshocks and mainshock. Red lines indicate estimated active faults (HERP, 2013).

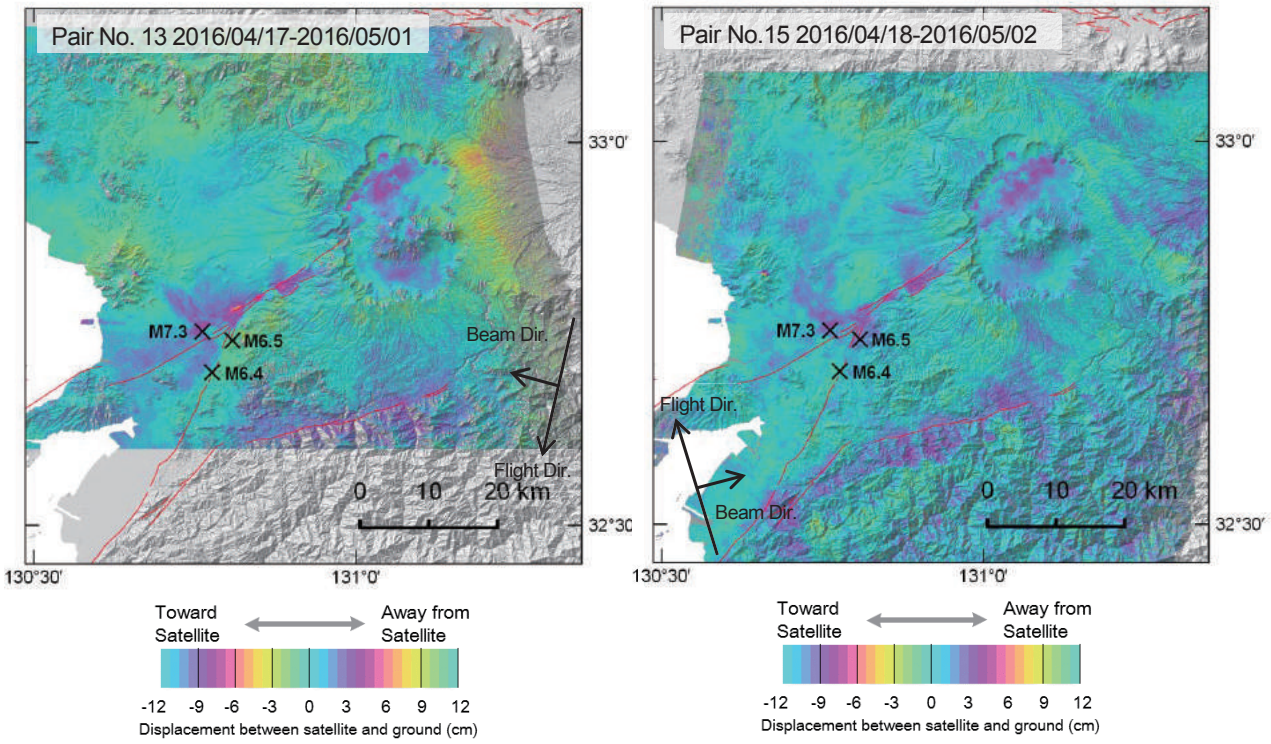

Fig. 3 SAR interferograms of pair No. 13 and No. 15. Black crosses indicate epicenters of the two foreshocks and mainshock. Red lines indicate estimated active faults (HERP, 2013).

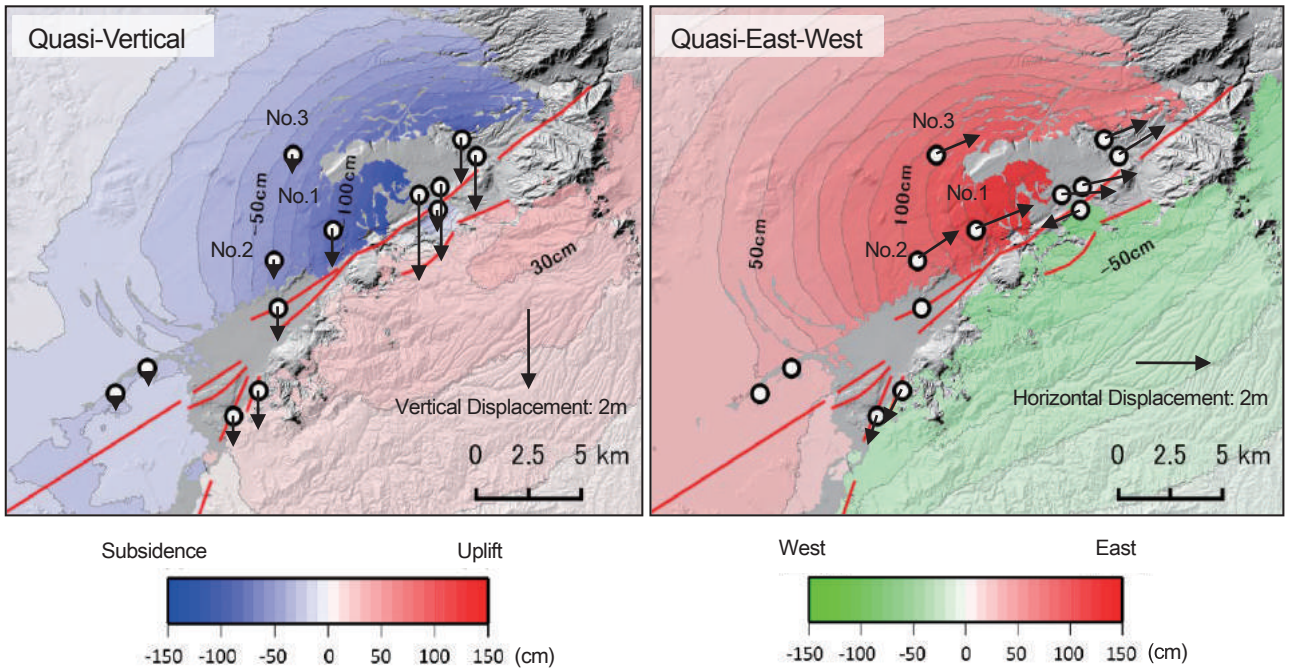

Fig. 4 2.5-D displacement filed estimated from SAR interferograms of pair No. 3 and No. 4. Open circles indicate locations of GNSS campaign observations. Red line indicates estimated active faults (HERP, 2013).

Table 2 Difference between InSAR 2.5-D displacements and GNSS

Station No.	Quasi-vertical displacement (cm)			Quasi-east-west displacement (cm)		
	2.5-D	GNSS	Difference	2.5-D	GNSS	Difference
1	−95.0	−103.0	8.0	129.9	148.1	−18.2
2	−62.3	−59.6	−2.7	100.3	104.3	−4.0
3	−55.7	−55.0	−0.7	106.4	111.7	−5.3

detailed crustal deformation all over Japan. Monitoring of ground surface movements will continue throughout Japan using interferograms of ALOS-2.

Acknowledgements

ALOS-2 data were provided from the Earthquake Working Group under a cooperative research contract with JAXA. The ownership of ALOS-2 data belongs to JAXA.

The earthquake catalogue and the numerical weather model were provided from JMA.

References

Fujiwara, S., T. Nishimura, M. Murakami, H. Nakagawa, M. Tobita and P.A. Rosen (2000): 2.5-D surface deformation of M6.1 earthquake near Mt Iwate detected by SAR interferometry. Geophys Res Lett 27:2049–2052.

Headquarters for Earthquake Research Promotion (2013): Evaluation of active faults to date. http://jishin.go.jp/main/chousa/katsudansou_pdf/93_futagawa_hinagu_2.pdf (accessed August 3, 2016). (in Japanese)

Japan Meteorological Agency (2016): Hypocenter map (2016 Kumamoto Earthquake). http://www.data.jma.go.jp/svd/eqev/data/2016_04_14_kumamoto/kouiki.pdf (accessed 6 June 2016). (in Japanese)

Kobayashi, T., M. Tobita, T. Nishimura, A. Suzuki, Y. Noguchi and M. Yamanaka (2011): Crustal deformation map for the 2011 off the Pacific coast of Tohoku Earthquake, detected by InSAR analysis combined with GEONET data. Earth Planets Space 63:621–625.

Kobayashi, T., M. Ishimoto, M. Tobita and H. Yarai (2014): A tool for reduction of atmosphere-related noises included in an InSAR image, incorporating a numerical weather model, Jour. GSI, 125, 31-38 (in Japanese)

Kobayashi, T. (2016): Earthquake rupture properties for foreshocks (M6.5 and M6.4) of the 2016 Kumamoto Earthquake, revealed by conventional and multiple-aperture InSAR, submitted to Earth, Planets and Space.

Morishita, Y. (2016): Reduction of Spatially Long Wavelength Noises in SAR Interferograms Using GNSS Data, J Geod Soc Jpn, in press (in Japanese with English abstract).

Morishita, Y., T. Kobayashi and H. Yarai (2016): Three-dimensional deformation mapping of a dike intrusion event in Sakurajima in 2015 by exploiting the right- and left-looking ALOS-2 InSAR. Geophys Res Lett 43:4197–4204.